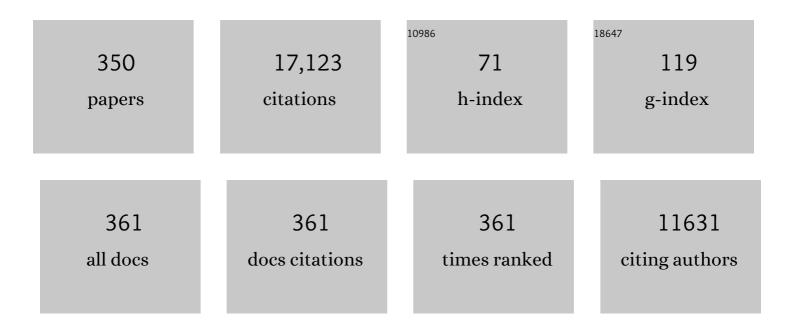
Maryellen Lissak Giger

List of Publications by Year in descending order

Source: https://exaly.com/author-pdf/230862/publications.pdf Version: 2024-02-01



#	Article	IF	CITATIONS
1	A review of explainable and interpretable AI with applications in COVIDâ€19 imaging. Medical Physics, 2022, 49, 1-14.	3.0	58
2	Deep learning to detect lymphocytes with high phenotypic resolution in highly multiplexed fluorescence microscopy images of triple-negative breast cancer biopsies. , 2022, , .		1
3	Association between DCE MRI background parenchymal enhancement and mammographic texture features. , 2022, , .		Ο
4	Case-based repeatability and operating point variability of AI: breast lesion classification based on deep transfer learning. , 2022, , .		0
5	Effect of different molecular subtype reference standards in Al training: implications for DCE-MRI radiomics of breast cancers. , 2022, , .		Ο
6	Advancing Research on Medical Image Perception by Strengthening Multidisciplinary Collaboration. JNCI Cancer Spectrum, 2022, 6, .	2.9	2
7	Machine Learning for Early Detection of Hypoxic-Ischemic Brain Injury After Cardiac Arrest. Neurocritical Care, 2022, 36, 974-982.	2.4	14
8	A machine-learning algorithm for distinguishing malignant from benign indeterminate thyroid nodules using ultrasound radiomic features. Journal of Medical Imaging, 2022, 9, .	1.5	9
9	Specific in situ inflammatory states associate with progression to renal failure in lupus nephritis. Journal of Clinical Investigation, 2022, 132, .	8.2	21
10	Performance metric curve analysis framework to assess impact of the decision variable threshold, disease prevalence, and dataset variability in two-class classification. Journal of Medical Imaging, 2022, 9, .	1.5	4
11	Impact of continuous learning on diagnostic breast MRI AI: evaluation on an independent clinical dataset. Journal of Medical Imaging, 2022, 9, .	1.5	0
12	Artificial intelligence and interpretations in breast cancer imaging. , 2021, , 291-308.		2
13	Special Report of the RSNA COVID-19 Task Force: The Short- and Long-term Financial Impact of the COVID-19 Pandemic on Private Radiology Practices. Radiology, 2021, 298, E11-E18.	7.3	20
14	Al/Machine Learning in Medical Imaging. , 2021, , 1691-1702.		3
15	Automated mesenchymal stem cell segmentation and machine learning-based phenotype classification using morphometric and textural analysis. Journal of Medical Imaging, 2021, 8, 014503.	1.5	15
16	Enhanced detection of oral dysplasia by structured illumination fluorescence lifetime imaging microscopy. Scientific Reports, 2021, 11, 4984.	3.3	2
17	Improved Classification of Benign and Malignant Breast Lesions Using Deep Feature Maximum Intensity Projection MRI in Breast Cancer Diagnosis Using Dynamic Contrast-enhanced MRI. Radiology: Artificial Intelligence, 2021, 3, e200159.	5.8	27
18	Anatomic Point–Based Lung Region with Zone Identification for Radiologist Annotation and Machine Learning for Chest Radiographs. Journal of Digital Imaging, 2021, 34, 922-931.	2.9	0

#	Article	IF	CITATIONS
19	Dual-energy three-compartment breast imaging for compositional biomarkers to improve detection of malignant lesions. Communications Medicine, 2021, 1, .	4.2	1
20	Role of standard and soft tissue chest radiography images in deep-learning-based early diagnosis of COVID-19. Journal of Medical Imaging, 2021, 8, 014503.	1.5	10
21	Multi-Stage Harmonization for Robust Al across Breast MR Databases. Cancers, 2021, 13, 4809.	3.7	6
22	Robustness of radiomic features of benign breast lesions and hormone receptor positive/HER2-negative cancers across DCE-MR magnet strengths. Magnetic Resonance Imaging, 2021, 82, 111-121.	1.8	3
23	Lessons learned in transitioning to AI in the medical imaging of COVID-19. Journal of Medical Imaging, 2021, 8, 010902-10902.	1.5	13
24	Artificial Intelligence and Cellular Segmentation in Tissue Microscopy Images. American Journal of Pathology, 2021, 191, 1693-1701.	3.8	30
25	Quantifying the effects of biopsy fixation and staining panel design on automatic instance segmentation of immune cells in human lupus nephritis. Journal of Biomedical Optics, 2021, 26, .	2.6	7
26	Artificial Intelligence in Medical Imaging. , 2021, , 1-22.		1
27	Clinical Artificial Intelligence Applications. Radiologic Clinics of North America, 2021, 59, 1027-1043.	1.8	12
28	Report from the RSNA COVID-19 Task Force: COVID-19 Impact on Academic Radiology Research- A Survey of Vice Chairs of Research. Journal of the American College of Radiology, 2021, , .	1.8	5
29	Artificial intelligence in the interpretation of breast cancer on MRI. Journal of Magnetic Resonance Imaging, 2020, 51, 1310-1324.	3.4	116
30	Comparison of Breast MRI Tumor Classification Using Human-Engineered Radiomics, Transfer Learning From Deep Convolutional Neural Networks, and Fusion Methods. Proceedings of the IEEE, 2020, 108, 163-177.	21.3	45
31	Tailoring steroids in the treatment of COVID-19 pneumonia assisted by CT scans: three case reports. Journal of X-Ray Science and Technology, 2020, 28, 885-892.	1.0	7
32	A deep learning methodology for improved breast cancer diagnosis using multiparametric MRI. Scientific Reports, 2020, 10, 10536.	3.3	86
33	Artificial Intelligence: reshaping the practice of radiological sciences in the 21st century. British Journal of Radiology, 2020, 93, 20190855.	2.2	63
34	Harmonization of radiomic features of breast lesions across international DCE-MRI datasets. Journal of Medical Imaging, 2020, 7, 1.	1.5	32
35	Deep convolutional neural networks in the classification of dual-energy thoracic radiographic views for efficient workflow: analysis on over 6500 clinical radiographs. Journal of Medical Imaging, 2020, 7, 1.	1.5	3
36	Radiomics methodology for breast cancer diagnosis using multiparametric magnetic resonance imaging. Journal of Medical Imaging, 2020, 7, 044502.	1.5	21

#	Article	IF	CITATIONS
37	Three compartment breast machine learning model for improving computer-aided detection. , 2020, , .		1
38	CT Texture Characterization. , 2020, , 319-329.		0
39	Cascaded deep transfer learning on thoracic CT in COVID-19 patients treated with steroids. Journal of Medical Imaging, 2020, 8, 014501.	1.5	6
40	Transfer Learning From Convolutional Neural Networks for Computer-Aided Diagnosis: A Comparison of Digital Breast Tomosynthesis and Full-Field Digital Mammography. Academic Radiology, 2019, 26, 735-743.	2.5	70
41	Additive Benefit of Radiomics Over Size Alone in the Distinction Between Benign Lesions and Luminal A Cancers on a Large Clinical Breast MRI Dataset. Academic Radiology, 2019, 26, 202-209.	2.5	41
42	Relationships Between Human-Extracted MRI Tumor Phenotypes of Breast Cancer and Clinical Prognostic Indicators Including Receptor Status and Molecular Subtype. Current Problems in Diagnostic Radiology, 2019, 48, 467-472.	1.4	11
43	Radiogenomics of breast cancer using dynamic contrast enhanced MRI and gene expression profiling. Cancer Imaging, 2019, 19, 48.	2.8	48
44	Independent validation of machine learning in diagnosing breast Cancer on magnetic resonance imaging within a single institution. Cancer Imaging, 2019, 19, 64.	2.8	41
45	Prognostic value of pre-treatment CT texture analysis in combination with change in size of the primary tumor in response to induction chemotherapy for HPV-positive oropharyngeal squamous cell carcinoma. Quantitative Imaging in Medicine and Surgery, 2019, 9, 399-408.	2.0	13
46	Artificial intelligence in cancer imaging: Clinical challenges and applications. Ca-A Cancer Journal for Clinicians, 2019, 69, 127-157.	329.8	965
47	Radiomics robustness assessment and classification evaluation: A twoâ€stage method demonstrated on multivendor <scp>FFDM</scp> . Medical Physics, 2019, 46, 2145-2156.	3.0	22
48	Quantifying in situ adaptive immune cell cognate interactions in humans. Nature Immunology, 2019, 20, 503-513.	14.5	26
49	Digital Mammography in Breast Cancer: Additive Value of Radiomics of Breast Parenchyma. Radiology, 2019, 291, 15-20.	7.3	66
50	Deep learning in medical imaging and radiation therapy. Medical Physics, 2019, 46, e1-e36.	3.0	513
51	Combined Benefit of Quantitative Three-Compartment Breast Image Analysis and Mammography Radiomics in the Classification of Breast Masses in a Clinical Data Set. Radiology, 2019, 290, 621-628.	7.3	29
52	Effect of biopsy on the MRI radiomics classification of benign lesions and luminal A cancers. Journal of Medical Imaging, 2019, 6, 1.	1.5	5
53	Breast MRI radiomics for the pretreatment prediction of response to neoadjuvant chemotherapy in node-positive breast cancer patients. Journal of Medical Imaging, 2019, 6, 1.	1.5	21
54	Evaluating deep learning techniques for dynamic contrast-enhanced MRI in the diagnosis of breast		7

Evaluating deep le cancer. , 2019, , .

#	Article	IF	CITATIONS
55	Impact of imprinted labels on deep learning classification of AP and PA thoracic radiographs. , 2019, , .		2
56	Breast MRI radiomics for the pre-treatment prediction of response to neoadjuvant chemotherapy in node-positive breast cancer patients. , 2019, , .		3
57	Effect of diversity of patient population and acquisition systems on the use of radiomics and machine learning for classification of 2,397 breast lesions. , 2019, , .		0
58	Radiomics and deep learning of diffusion-weighted MRI in the diagnosis of breast cancer. , 2019, , .		3
59	Temporal mammographic registration for evaluation of architecture changes in cancer risk assessment. , 2019, , .		2
60	Most-enhancing tumor volume by MRI radiomics predicts recurrence-free survival "early on―in neoadjuvant treatment of breast cancer. Cancer Imaging, 2018, 18, 12.	2.8	51
61	Machine Learning in Medical Imaging. Journal of the American College of Radiology, 2018, 15, 512-520.	1.8	383
62	A brief history of the <scp>AAPM</scp> : Celebrating 60 years of contributions to medical physics practice and science. Medical Physics, 2018, 45, 497-501.	3.0	1
63	CAD: An Image Perception Perspective. , 2018, , 359-373.		0
64	Opportunities and challenges to utilization of quantitative imaging: Report of the <scp>AAPM</scp> practical big data workshop. Medical Physics, 2018, 45, e820-e828.	3.0	7
65	Special Section Guest Editorial: Radiomics and Deep Learning. Journal of Medical Imaging, 2018, 4, 1.	1.5	12
66	Fuzzy c-means segmentation of major vessels in angiographic images of stroke. Journal of Medical Imaging, 2018, 5, 1.	1.5	3
67	Use of clinical MRI maximum intensity projections for improved breast lesion classification with deep convolutional neural networks. Journal of Medical Imaging, 2018, 5, 1.	1.5	54
68	PROSTATEx Challenges for computerized classification of prostate lesions from multiparametric magnetic resonance images. Journal of Medical Imaging, 2018, 5, 1.	1.5	98
69	Variation in algorithm implementation across radiomics software. Journal of Medical Imaging, 2018, 5, 1.	1.5	60
70	Breast lesion classification based on dynamic contrast-enhanced magnetic resonance images sequences with long short-term memory networks. Journal of Medical Imaging, 2018, 6, 1.	1.5	13
71	Recurrent neural networks for breast lesion classification based on DCE-MRIs. , 2018, , .		1
72	Robustness of radiomic breast features of benign lesions and luminal A cancers across MR magnet strengths. , 2018, , .		5

#	Article	IF	CITATIONS
73	Deep learning in breast cancer risk assessment: evaluation of fine-tuned convolutional neural neural networks on a clinical dataset of FFDMs. , 2018, , .		1
74	Transfer learning with convolutional neural networks for lesion classification on clinical breast tomosynthesis. , 2018, , .		4
75	Deep learning in computer-aided diagnosis incorporating mammographic characteristics of both tumor and parenchyma stroma. , 2018, , .		1
76	Variations in algorithm implementation among quantitative texture analysis software packages. , 2018, , .		0
77	Temporal assessment of radiomic features on clinical mammography in a high-risk population. , 2018, , .		0
78	Radiomics for ultrafast dynamic contrast-enhanced breast MRI in the diagnosis of breast cancer: a pilot study. , 2018, , .		0
79	Effect of biopsy on the MRI radiomics classification of benign lesions and luminal A cancers. , 2018, , .		0
80	Performance comparison of deep learning and segmentation-based radiomic methods in the task of distinguishing benign and malignant breast lesions on DCE-MRI. Proceedings of SPIE, 2017, , .	0.8	7
81	Deep learning and three-compartment breast imaging in breast cancer diagnosis. Proceedings of SPIE, 2017, , .	0.8	1
82	Fast bilateral breast coverage with high spectral and spatial resolution (HiSS) MRI at 3T. Journal of Magnetic Resonance Imaging, 2017, 46, 1341-1348.	3.4	8
83	Letter to the Editor. Academic Radiology, 2017, 24, 916-917.	2.5	0
84	A deep feature fusion methodology for breast cancer diagnosis demonstrated on three imaging modality datasets. Medical Physics, 2017, 44, 5162-5171.	3.0	292
85	Lightâ€Based Technologies for a Better World. Optik & Photonik, 2017, 12, 1-1.	0.2	0
86	Breast MRI radiomics: comparison of computer- and human-extracted imaging phenotypes. European Radiology Experimental, 2017, 1, 22.	3.4	29
87	Deep learning in breast cancer risk assessment: evaluation of convolutional neural networks on a clinical dataset of full-field digital mammograms. Journal of Medical Imaging, 2017, 4, 1.	1.5	53
88	Quantitative texture analysis: robustness of radiomics across two digital mammography manufacturers' systems. Journal of Medical Imaging, 2017, 5, 1.	1.5	11
89	Bclâ€2 as a Therapeutic Target in Human Tubulointerstitial Inflammation. Arthritis and Rheumatology, 2016, 68, 2740-2751.	5.6	22
90	Using computerâ€extracted image phenotypes from tumors on breast magnetic resonance imaging to predict breast cancer pathologic stage. Cancer, 2016, 122, 748-757.	4.1	58

#	Article	IF	CITATIONS
91	Breast density estimation from high spectral and spatial resolution MRI. Journal of Medical Imaging, 2016, 3, 044507.	1.5	9
92	LUNGx Challenge for computerized lung nodule classification. Journal of Medical Imaging, 2016, 3, 044506.	1.5	80
93	Automated Breast Ultrasound in Breast Cancer Screening of Women With Dense Breasts: Reader Study of Mammography-Negative and Mammography-Positive Cancers. American Journal of Roentgenology, 2016, 206, 1341-1350.	2.2	85
94	MR Imaging Radiomics Signatures for Predicting the Risk of Breast Cancer Recurrence as Given by Research Versions of MammaPrint, Oncotype DX, and PAM50 Gene Assays. Radiology, 2016, 281, 382-391.	7.3	387
95	Identification, segmentation, and characterization of microcalcifications on mammography. , 2016, , .		0
96	Clinical significance of noncalcified lung nodules in patients with breast cancer. Breast Cancer Research and Treatment, 2016, 159, 265-271.	2.5	8
97	Digital mammographic tumor classification using transfer learning from deep convolutional neural networks. Journal of Medical Imaging, 2016, 3, 034501.	1.5	391
98	Quantitative MRI radiomics in the prediction of molecular classifications of breast cancer subtypes in the TCGA/TCIA data set. Npj Breast Cancer, 2016, 2, .	5.2	266
99	Energy Dependence of Water and Lipid Calibration Materials for Three-Compartment Breast Imaging. Lecture Notes in Computer Science, 2016, , 554-563.	1.3	1
100	Deciphering Genomic Underpinnings of Quantitative MRI-based Radiomic Phenotypes of Invasive Breast Carcinoma. Scientific Reports, 2015, 5, 17787.	3.3	134
101	Quantitative imaging biomarkers: A review of statistical methods for computer algorithm comparisons. Statistical Methods in Medical Research, 2015, 24, 68-106.	1.5	137
102	Dual-Lumen Chest Port Infection Rates in Patients with Head and Neck Cancer. CardioVascular and Interventional Radiology, 2015, 38, 651-656.	2.0	6
103	Guest Editorial: LUNGx Challenge for computerized lung nodule classification: reflections and lessons learned. Journal of Medical Imaging, 2015, 2, 020103.	1.5	51
104	Special Section Guest Editorial:Radiomics and Imaging Genomics: Quantitative Imaging for Precision Medicine. Journal of Medical Imaging, 2015, 2, 041001.	1.5	17
105	Preliminary assessment of dispersion versus absorption analysis of high spectral and spatial resolution magnetic resonance images in the diagnosis of breast cancer. Journal of Medical Imaging, 2015, 2, 024502.	1.5	4
106	Using quantitative image analysis to classify axillary lymph nodes on breast MRI: A new application for the Z 0011 Era. European Journal of Radiology, 2015, 84, 392-397.	2.6	28
107	Prediction of clinical phenotypes in invasive breast carcinomas from the integration of radiomics and genomics data. Journal of Medical Imaging, 2015, 2, 041007.	1.5	126
108	Manganeseâ€enhanced MRI detection of impaired calcium regulation in a mouse model of cardiac hypertrophy. NMR in Biomedicine, 2015, 28, 255-263.	2.8	7

#	Article	IF	CITATIONS
109	Medical imaging and computers in the diagnosis of breast cancer. Proceedings of SPIE, 2014, , .	0.8	4
110	Compositional Three-Component Breast Imaging of Fibroadenoma and Invasive Cancer Lesions: Pilot Study. Lecture Notes in Computer Science, 2014, , 109-114.	1.3	1
111	Roles of biologic breast tissue composition and quantitative image analysis of mammographic images in breast tumor characterization. , 2014, , .		Ο
112	Comparative analysis of image-based phenotypes of mammographic density and parenchymal patterns in distinguishing between <i>BRCA1/2</i> cases, unilateral cancer cases, and controls. Journal of Medical Imaging, 2014, 1, 031009.	1.5	31
113	Impact of lesion segmentation metrics on computer-aided diagnosis/detection in breast computed tomography. Journal of Medical Imaging, 2014, 1, 031012.	1.5	8
114	Validation of Quantitative Analysis of Multiparametric Prostate MR Images for Prostate Cancer Detection and Aggressiveness Assessment: A Cross-Imager Study. Radiology, 2014, 271, 461-471.	7.3	72
115	Pilot study demonstrating potential association between breast cancer imageâ€based risk phenotypes and genomic biomarkers. Medical Physics, 2014, 41, 031917.	3.0	21
116	Residual analysis of the water resonance signal in breast lesions imaged with high spectral and spatial resolution (HiSS) MRI: A pilot study. Medical Physics, 2014, 41, 012303.	3.0	14
117	Potential of computerâ€aided diagnosis of high spectral and spatial resolution (HiSS) MRI in the classification of breast lesions. Journal of Magnetic Resonance Imaging, 2014, 39, 59-67.	3.4	22
118	Mammographic quantitative image analysis and biologic image composition for breast lesion characterization and classification. Medical Physics, 2014, 41, 031915.	3.0	15
119	Relationships between computer-extracted mammographic texture pattern features and BRCA1/2mutation status: a cross-sectional study. Breast Cancer Research, 2014, 16, 424.	5.0	44
120	Cell Distance Mapping Identifies Functional T Follicular Helper Cells in Inflamed Human Renal Tissue. Science Translational Medicine, 2014, 6, 230ra46.	12.4	162
121	Segmentation of breast masses on dedicated breast computed tomography and three-dimensional breast ultrasound images. Journal of Medical Imaging, 2014, 1, 014501.	1.5	18
122	Level Set Segmentation of Breast Masses in Contrast-Enhanced Dedicated Breast CT and Evaluation of Stopping Criteria. Journal of Digital Imaging, 2014, 27, 237-247.	2.9	23
123	Comparison of Barbed versus Conventional Sutures for Wound Closure of Radiologically Implanted Chest Ports. Journal of Vascular and Interventional Radiology, 2014, 25, 1433-1438.	0.5	7
124	Quantitative MRI Phenotyping of Breast Cancer across Molecular Classification Subtypes. Lecture Notes in Computer Science, 2014, , 195-200.	1.3	3
125	Relationships between computer-extracted mammographic texture pattern features and. Breast Cancer Research, 2014, 16, 424.	5.0	21
126	Quantitative ultrasound image analysis of axillary lymph node status in breast cancer patients. International Journal of Computer Assisted Radiology and Surgery, 2013, 8, 895-903.	2.8	14

#	Article	IF	CITATIONS
127	Interreader Scoring Variability in an Observer Study Using Dual-Modality Imaging for Breast Cancer Detection in Women with Dense Breasts. Academic Radiology, 2013, 20, 847-853.	2.5	17
128	Breast Image Analysis for Risk Assessment, Detection, Diagnosis, and Treatment of Cancer. Annual Review of Biomedical Engineering, 2013, 15, 327-357.	12.3	175
129	A study of T2-weighted MR image texture features and diffusion-weighted MR image features for computer-aided diagnosis of prostate cancer. , 2013, , .		19
130	Automatic 3D lesion segmentation on breast ultrasound images. Proceedings of SPIE, 2013, , .	0.8	3
131	Quantitative Analysis of Multiparametric Prostate MR Images: Differentiation between Prostate Cancer and Normal Tissue and Correlation with Gleason Score—A Computer-aided Diagnosis Development Study. Radiology, 2013, 267, 787-796.	7.3	229
132	Computerized detection of breast cancer on automated breast ultrasound imaging of women with dense breasts. Medical Physics, 2013, 41, 012901.	3.0	20
133	Ethics and professionalism in medical physics: A survey of AAPM members. Medical Physics, 2013, 40, 047001.	3.0	14
134	Re: Effectiveness of Computer-Aided Detection in Community Mammography Practice. Journal of the National Cancer Institute, 2012, 104, 77-77.	6.3	3
135	Computerized image analysis of cell-cell interactions in human renal tissue by using multi-channel immunoflourescent confocal microscopy. , 2012, , .		0
136	Breast image feature learning with adaptive deconvolutional networks. Proceedings of SPIE, 2012, , .	0.8	31
137	Computerized Analysis of Mammographic Parenchymal Patterns on a Large Clinical Dataset of Full-Field Digital Mammograms: Robustness Study with Two High-Risk Datasets. Journal of Digital Imaging, 2012, 25, 591-598.	2.9	41
138	Research Imaging in an Academic Medical Center. Academic Radiology, 2012, 19, 762-771.	2.5	6
139	A scaling transformation for classifier output based on likelihood ratio: Applications to a CAD workstation for diagnosis of breast cancer. Medical Physics, 2012, 39, 2787-2804.	3.0	8
140	Level Set Breast Mass Segmentation in Contrast-Enhanced and Non-Contrast-Enhanced Breast CT. Lecture Notes in Computer Science, 2012, , 697-704.	1.3	2
141	Robustness Studies of Ultrasound CADx in Breast Cancer Diagnosis. Advances in Bioinformatics and Biomedical Engineering Book Series, 2012, , 1-22.	0.4	0
142	Exploring deep parametric embeddings for breast CADx. , 2011, , .		2
143	Comparison of two-class and three-class Bayesian artificial neural networks in estimation of observations drawn from simulated bivariate normal distributions. Proceedings of SPIE, 2011, , .	0.8	0
144	Normal parenchymal enhancement patterns in women undergoing MR screening of the breast. European Radiology, 2011, 21, 1374-1382.	4.5	38

#	Article	IF	CITATIONS
145	Combined use of <i>T</i> ₂ â€weighted MRI and <i>T</i> ₁ â€weighted dynamic contrast–enhanced MRI in the automated analysis of breast lesions. Magnetic Resonance in Medicine, 2011, 66, 555-564.	3.0	34
146	Computerized three-class classification of MRI-based prognostic markers for breast cancer. Physics in Medicine and Biology, 2011, 56, 5995-6008.	3.0	35
147	Evaluation of Clinical Breast MR Imaging Performed with Prototype Computer-aided Diagnosis Breast MR Imaging Workstation: Reader Study. Radiology, 2011, 258, 696-704.	7.3	37
148	Exploring nonlinear feature space dimension reduction and data representation in breast CADx with Laplacian eigenmaps and NE. Medical Physics, 2010, 37, 339-351.	3.0	118
149	Optimization of a fuzzy C-means approach to determining probability of lesion malignancy and quantifying lesion enhancement heterogeneity in breast DCE-MRI. , 2010, , .		0
150	Repeatability in computerâ€aided diagnosis: Application to breast cancer diagnosis on sonography. Medical Physics, 2010, 37, 2659-2669.	3.0	17
151		3.0	18
152	Computerized method for evaluating diagnostic image quality of calcified plaque images in cardiac CT: Validation on a physical dynamic cardiac phantom. Medical Physics, 2010, 37, 5777-5786.	3.0	3
153	Effect of variable gain on computerized texture analysis on digitalized mammograms. , 2010, , .		1
154	Radiographic texture analysis of densitometric calcaneal images: Relationship to clinical characteristics and to bone fragility. Journal of Bone and Mineral Research, 2010, 25, 56-63.	2.8	23
155	A Novel Hybrid Linear/Nonlinear Classifier for Two-Class Classification: Theory, Algorithm, and Applications. IEEE Transactions on Medical Imaging, 2010, 29, 428-441.	8.9	11
156	Update on the potential of computer-aided diagnosis for breast cancer. Future Oncology, 2010, 6, 1-4.	2.4	24
157	Cancerous Breast Lesions on Dynamic Contrast-enhanced MR Images: Computerized Characterization for Image-based Prognostic Markers. Radiology, 2010, 254, 680-690.	7.3	172
158	Computerized Assessment of Breast Lesion Malignancy using DCE-MRI. Academic Radiology, 2010, 17, 822-829.	2.5	47
159	Multimodality Computer-Aided Breast Cancer Diagnosis with FFDM and DCE-MRI. Academic Radiology, 2010, 17, 1158-1167.	2.5	50
160	Performance of Triple-Modality CADx on Breast Cancer Diagnostic Classification. Lecture Notes in Computer Science, 2010, , 9-14.	1.3	1
161	Validation of Mammographic Texture Analysis for Assessment of Breast Cancer Risk. Lecture Notes in Computer Science, 2010, , 267-271.	1.3	3
162	Breast US Computer-aided Diagnosis System: Robustness across Urban Populations in South Korea and the United States. Radiology, 2009, 253, 661-671.	7.3	24

#	Article	IF	CITATIONS
163	Automated Method for Improving System Performance of Computer-Aided Diagnosis in Breast Ultrasound. IEEE Transactions on Medical Imaging, 2009, 28, 122-128.	8.9	34
164	Breast cancer classification with mammography and DCE-MRI. , 2009, , .		0
165	Using three-class BANN classifier in the automated analysis of breast cancer lesions in DCE-MRI. , 2009, , .		1
166	Computerized breast parenchymal analysis on DCE-MRI. , 2009, , .		2
167	Temporal radiographic texture analysis in the detection of periprosthetic osteolysis. Medical Physics, 2008, 35, 377-387.	3.0	6
168	Power Spectral Analysis of Mammographic Parenchymal Patterns for Breast Cancer Risk Assessment. Journal of Digital Imaging, 2008, 21, 145-152.	2.9	51
169	Evaluation of Computer-aided Diagnosis on a Large Clinical Full-field Digital Mammographic Dataset. Academic Radiology, 2008, 15, 1437-1445.	2.5	33
170	Prevalence Scaling. Academic Radiology, 2008, 15, 1446-1457.	2.5	21
171	Radiographic Texture Analysis in the Characterization of Trabecular Patterns in Periprosthetic Osteolysis. Academic Radiology, 2008, 15, 176-185.	2.5	7
172	Performance of Breast Ultrasound Computer-aided Diagnosis. Academic Radiology, 2008, 15, 1234-1245.	2.5	29
173	Potential Effect of Different Radiologist Reporting Methods on Studies Showing Benefit of CAD. Academic Radiology, 2008, 15, 139-152.	2.5	16
174	Reproducibility and Sources of Variability in Radiographic Texture Analysis of Densitometric Calcaneal Images. Journal of Clinical Densitometry, 2008, 11, 211-220.	1.2	8
175	Correlative feature analysis of FFDM images. Proceedings of SPIE, 2008, , .	0.8	5
176	Chord-based image reconstruction from clinical projection data. , 2008, , .		1
177	Computerized assessment of coronary calcified plaques in CT images of a dynamic cardiac phantom. , 2008, , .		1
178	Breast US Computer-aided Diagnosis Workstation: Performance with a Large Clinical Diagnostic Population. Radiology, 2008, 248, 392-397.	7.3	49
179	Hybrid linear classifier for jointly normal data: theory. Proceedings of SPIE, 2008, , .	0.8	1
180	Anniversary Paper: History and status of CAD and quantitative image analysis: The role of <i>Medical Physics</i> and AAPM. Medical Physics, 2008, 35, 5799-5820.	3.0	250

#	Article	IF	CITATIONS
181	DCEMRI of breast lesions: Is kinetic analysis equally effective for both mass and nonmass-like enhancement?. Medical Physics, 2008, 35, 3102-3109.	3.0	58
182	Correlative feature analysis on FFDM. Medical Physics, 2008, 35, 5490-5500.	3.0	15
183	Computer-Aided Diagnosis. , 2008, , 359-XXII.		23
184	Identifying Corresponding Lesions from CC and MLO Views Via Correlative Feature Analysis. Lecture Notes in Computer Science, 2008, , 323-328.	1.3	4
185	Performance of CADx on a Large Clinical Database of FFDM Images. Lecture Notes in Computer Science, 2008, , 510-514.	1.3	2
186	Image quality evaluation of motion-contaminated calcified plaques in cardiac CT. , 2007, , .		0
187	The effect of image quality on the appearance of lesions on breast ultrasound: implications for CADx. , 2007, 6514, 433.		2
188	Computerized assessment of motionâ€contaminated calcified plaques in cardiac multidetector CT. Medical Physics, 2007, 34, 4876-4889.	3.0	8
189	Featureâ€based characterization of motionâ€contaminated calcified plaques in cardiac multidetector CT. Medical Physics, 2007, 34, 4860-4875.	3.0	7
190	PROGRESS IN BREAST CADx., 2007, , .		2
191	A dualâ€stage method for lesion segmentation on digital mammograms. Medical Physics, 2007, 34, 4180-4193.	3.0	92
192	Imputation methods for temporal radiographic texture analysis in the detection of periprosthetic osteolysis. , 2007, , .		2
193	An image database management system for conducting CAD research. , 2007, , .		0
194	Automatic selection of region of interest for radiographic texture analysis. , 2007, , .		2
195	Motion compensated reconstructions of calcified coronary plaques in cardiac CT. , 2007, , .		0
196	Joint feature selection and classification using a Bayesian neural network with automatic relevance determination priors: potential use in CAD of medical imaging. , 2007, , .		3
197	Computer-aided assessment of cardiac computed tomographic images. , 2007, , .		0
198	Fractal Analysis of Mammographic Parenchymal Patterns in Breast Cancer Risk Assessment. Academic Radiology, 2007, 14, 513-521.	2.5	86

#	Article	IF	CITATIONS
199	Volumetric texture analysis of breast lesions on contrastâ€enhanced magnetic resonance images. Magnetic Resonance in Medicine, 2007, 58, 562-571.	3.0	270
200	Automatic identification and classification of characteristic kinetic curves of breast lesions on DCE-MRI. Medical Physics, 2006, 33, 2878-2887.	3.0	184
201	A Fuzzy C-Means (FCM)-Based Approach for Computerized Segmentation of Breast Lesions in Dynamic Contrast-Enhanced MR Images1. Academic Radiology, 2006, 13, 63-72.	2.5	316
202	Suppression of motion-induced streak artifacts along chords in fan-beam BPF-reconstructions of motion-contaminated projection data. , 2006, 6142, 725.		1
203	A novel strategy for segmentation of magnetic resonance (MR) images corrupted by intensity inhomogeneity artifacts. , 2006, , .		0
204	Investigation of Calcified Coronary Plaque Tracking in Cardiac CT. , 2006, , .		2
205	A two-stage method for lesion segmentation on digital mammograms. , 2006, , .		1
206	Power spectral analysis of mammographic parenchymal patterns. , 2006, , .		1
207	Investigation of temporal radiographic texture analysis for the detection of periprosthetic osteolysis. , 2006, 6144, 2212.		3
208	Classification of Breast Lesions with Multimodality Computer-aided Diagnosis: Observer Study Results on an Independent Clinical Data Set. Radiology, 2006, 240, 357-368.	7.3	98
209	Region-of-interest reconstruction of motion-contaminated data using a weighted backprojection filtration algorithm. Medical Physics, 2006, 33, 1222-1238.	3.0	9
210	Computerized mass detection for digital breast tomosynthesis directly from the projection images. Medical Physics, 2006, 33, 482-491.	3.0	85
211	Comparison of Computerized Image Analyses for Digitized Screen-Film Mammograms and Full-Field Digital Mammography Images. Lecture Notes in Computer Science, 2006, , 569-575.	1.3	3
212	Character recognition and image manipulation for the clinical translation of CAD for breast ultrasound. , 2005, 5747, 1128.		0
213	Robustness of Computerized Lesion Detection and Classification Scheme across Different Breast US Platforms. Radiology, 2005, 237, 834-840.	7.3	58
214	Update On the Potential Role of CAD in Radiologic Interpretations. Academic Radiology, 2005, 12, 669-670.	2.5	12
215	Computerized Texture Analysis of Mammographic Parenchymal Patterns of Digitized Mammograms1. Academic Radiology, 2005, 12, 863-873.	2.5	103
216	Multimodality Computerized Diagnosis of Breast Lesions Using Mammography and Sonography1. Academic Radiology, 2005, 12, 970-979.	2.5	38

#	Article	IF	CITATIONS
217	Investigation of physical image quality indices of a bone densitometry system. Medical Physics, 2004, 31, 873-881.	3.0	8
218	Comparison of radiographic texture analysis from computed radiography and bone densitometry systems. Medical Physics, 2004, 31, 882-891.	3.0	29
219	Computerized analysis of mammographic parenchymal patterns for assessing breast cancer risk: Effect of ROI size and location. Medical Physics, 2004, 31, 549-555.	3.0	96
220	Computerized interpretation of breast MRI: Investigation of enhancement-variance dynamics. Medical Physics, 2004, 31, 1076-1082.	3.0	169
221	Performance of computer-aided diagnosis in the interpretation of lesions on breast sonography. Academic Radiology, 2004, 11, 272-280.	2.5	87
222	Computerized detection and classification of cancer on breast ultrasound1. Academic Radiology, 2004, 11, 526-535.	2.5	98
223	Computerized texture analysis of mammographic parenchymal patterns of digitized mammograms. International Congress Series, 2004, 1268, 878-881.	0.2	12
224	Computerized analysis of images in the detection and diagnosis of breast cancer. Seminars in Ultrasound, CT and MRI, 2004, 25, 411-418.	1.5	70
225	A reconstruction-independent method for computerized mass detection in digital tomosynthesis images of the breast. , 2004, , .		4
226	Correlation of lesions from multiple images for CAD. , 2004, 5370, 93.		0
227	Automated identification of temporal pattern with high initial enhancement in dynamic MR lesions using fuzzy c-means algorithm. , 2004, 5370, 607.		2
228	Computerized detection and 3-way classification of breast lesions on ultrasound images. , 2004, , .		5
229	Estimating three-class ideal observer decision variables for computerized detection and classification of mammographic mass lesions. Medical Physics, 2003, 31, 81-90.	3.0	27
230	Computerized analysis of shadowing on breast ultrasound for improved lesion detection. Medical Physics, 2003, 30, 1833-1842.	3.0	44
231	Comparison of approaches for risk-modulated CAD. , 2003, , .		0
232	Computerized analysis of mammographic parenchymal patterns using fractal analysis. , 2003, 5032, 90.		1
233	Bayesian ANN estimates of three-class ideal observer decision variables for classification of mammographic masses. , 2003, 5034, 474.		2
234	Computerized detection and classification of lesions on breast ultrasound. , 2003, 5032, 106.		2

#	Article	IF	CITATIONS
235	Results of an Observer Study with an Intelligent Mammographic Workstation for CAD. , 2003, , 297-303.		9
236	Computerized Analysis of Digitized Mammograms of BRCA1 and BRCA2 Gene Mutation Carriers. Radiology, 2002, 225, 519-526.	7.3	119
237	Breast Cancer: Effectiveness of Computer-aided Diagnosis—Observer Study with Independent Database of Mammograms. Radiology, 2002, 224, 560-568.	7.3	138
238	Computerized analysis of sonograms for the detection of breast lesions. , 2002, 4684, 1320.		2
239	Lung Cancer: Performance of Automated Lung Nodule Detection Applied to Cancers Missed in a CT Screening Program. Radiology, 2002, 225, 685-692.	7.3	264
240	Optimizing feature selection across a multimodality database in computerized classification of breast lesions. , 2002, 4684, 986.		2
241	Investigation of using bone texture analysis on bone densitometry images. , 2002, 4684, 860.		2
242	Computerized Detection of Lung Nodules. , 2002, , .		0
243	Effect of case mix on feature selection in the computerized classification of mammographic lesions. , 2002, , .		2
244	Computerized lesion detection on breast ultrasound. Medical Physics, 2002, 29, 1438-1446.	3.0	186
245	Computerized diagnosis of breast lesions on ultrasound. Medical Physics, 2002, 29, 157-164.	3.0	183
246	Intelligent CAD workstation for breast imaging using similarity to known lesions and multiple visual prompt aids. , 2002, 4684, 768.		36
247	Computer-Aided Diagnosis in Radiology. Academic Radiology, 2002, 9, 1-3.	2.5	67
248	Automated detection of lung nodules in CT scans: Preliminary results. Medical Physics, 2001, 28, 1552-1561.	3.0	217
249	Ideal observer approximation using Bayesian classification neural networks. IEEE Transactions on Medical Imaging, 2001, 20, 886-899.	8.9	85
250	<title>Can computer-aided diagnosis (CAD) help radiologists find mammographically missed screening cancers?</title> . , 2001, 4324, 56.		3
251	<title>Computerized lung nodule detection: comparison of performance for low-dose and standard-dose helical CT scans</title> . , 2001, , .		8
252	<title>Computer-aided diagnosis of lesions on multimodality images of the breast</title> . , 2001, 4322, 656.		2

#	Article	IF	CITATIONS
253	<title>Analysis of computer-aided diagnosis on radiologists' performance using an independent
database</title> . , 2001, 4324, 45.		2
254	Guest editorial computer-aided diagnosis in medical imaging. IEEE Transactions on Medical Imaging, 2001, 20, 1205-1208.	8.9	112
255	Automatic segmentation of breast lesions on ultrasound. Medical Physics, 2001, 28, 1652-1659.	3.0	159
256	<title>Analysis of a three-dimensional lung nodule detection method for thoracic CT scans</title> . , 2000, 3979, 103.		9
257	<title>Evaluation of an automated segmentation method based on performances of an automated classification method</title> . , 2000, 3981, 16.		10
258	Computerized analysis of mammographic parenchymal patterns for breast cancer risk assessment: Feature selection. Medical Physics, 2000, 27, 4-12.	3.0	78
259	Computerized analysis of radiographic bone patterns: Effect of imaging conditions on performance. Medical Physics, 2000, 27, 75-85.	3.0	16
260	Normalized BMD as a predictor of bone strength. Academic Radiology, 2000, 7, 33-39.	2.5	15
261	Computerized classification of benign and malignant masses on digitized mammograms: A study of robustness. Academic Radiology, 2000, 7, 1077-1084.	2.5	71
262	COMPUTER-AIDED DETECTION AND DIAGNOSIS OF BREAST CANCER. Radiologic Clinics of North America, 2000, 38, 725-740.	1.8	80
263	Automated registration of frontal and lateral radionuclide lung scans with digital chest radiographs. Academic Radiology, 2000, 7, 530-539.	2.5	3
264	<title>Three-dimensional approach to lung nodule detection in helical CT</title> . , 1999, , .		19
265	Effect of dominant features on neural network performance in the classification of mammographic lesions. Physics in Medicine and Biology, 1999, 44, 2579-2595.	3.0	24
266	Computerized radiographic texture measures for characterizing bone strength: A simulated clinical setup using femoral neck specimens. Medical Physics, 1999, 26, 2295-2300.	3.0	23
267	Characterization of bone quality using computer-extracted radiographic features. Medical Physics, 1999, 26, 872-879.	3.0	29
268	Feature selection with limited datasets. Medical Physics, 1999, 26, 2176-2182.	3.0	46
269	Computerized Detection of Pulmonary Nodules on CT Scans. Radiographics, 1999, 19, 1303-1311.	3.3	343
270	Computerized analysis of abnormal asymmetry in digital chest radiographs: Evaluation of potential utility. Journal of Digital Imaging, 1999, 12, 34-42.	2.9	3

#	Article	IF	CITATIONS
271	Computerized analysis of lesions in US images of the breast. Academic Radiology, 1999, 6, 665-674.	2.5	63
272	Improving breast cancer diagnosis with computer-aided diagnosis. Academic Radiology, 1999, 6, 22-33.	2.5	306
273	Automated lung segmentation in digitized posteroanterior chest radiographs. Academic Radiology, 1998, 5, 245-255.	2.5	89
274	Computerized delineation and analysis of costophrenic angles in digital chest radiographs. Academic Radiology, 1998, 5, 329-335.	2.5	17
275	Automated computerized classification of malignant and benign masses on digitized mammograms. Academic Radiology, 1998, 5, 155-168.	2.5	178
276	Automated lung segmentation in digital lateral chest radiographs. Medical Physics, 1998, 25, 1507-1520.	3.0	25
277	Computerized analysis of breast lesions in three dimensions using dynamic magnetic-resonance imaging. Medical Physics, 1998, 25, 1647-1654.	3.0	171
278	<title>Automated detection of pulmonary nodules in helical computed tomography images of the thorax</title> . , 1998, 3338, 916.		9
279	<title>Automated feature extraction and classification of breast lesions in magnetic resonance
images</title> . , 1998, , .		3
280	Prospective Testing of a Clinical Mammography Workstation for CAD: Analysis of the First 10,000 Cases. Computational Imaging and Vision, 1998, , 401-406.	0.6	4
281	Computer-Aided Diagnosis of Digital Mammography and Ultrasound Images of Breast Mass Lesions. Computational Imaging and Vision, 1998, , 143-147.	0.6	1
282	Benefits of Computer-Aided Diagnosis (CAD) in Mammographic Diagnosis of Malignant and Benign Clustered Microcalcifications. Computational Imaging and Vision, 1998, , 215-220.	0.6	1
283	<title>Adaptive feature analysis of false positives for computerized detection of lung nodules in digital chest images</title> . , 1997, , .		5
284	Automated registration of ventilation-perfusion images with digital chest radiographs. Academic Radiology, 1997, 4, 183-192.	2.5	10
285	Development of an improved CAD scheme for automated detection of lung nodules in digital chest images. Medical Physics, 1997, 24, 1395-1403.	3.0	132
286	Computer aided diagnosis of breast cancer on mammograms. Breast Cancer, 1997, 4, 228-233.	2.9	26
287	An improved computer-assisted diagnostic scheme using wavelet transform for detecting clustered microcalcifications in digital mammograms. Academic Radiology, 1996, 3, 621-627.	2.5	83
288	<title>Signal/background separation by wavelet packets for detection of microcalcifications in mammograms</title> ., 1996,,.		10

17

#	Article	IF	CITATIONS
289	An improved shift-invariant artificial neural network for computerized detection of clustered microcalcifications in digital mammograms. Medical Physics, 1996, 23, 595-601.	3.0	98
290	<title>Initial experience with a prototype clinical intelligent mammography workstation for computer-aided diagnosis</title> . , 1995, , .		13
291	Potential usefulness of digital imaging in clinical diagnostic radiology: Computer-aided diagnosis. Journal of Digital Imaging, 1995, 8, 2-7.	2.9	12
292	Detection of lung nodules in digital chest radiographs using artificial neural networks: A pilot study. Journal of Digital Imaging, 1995, 8, 88-94.	2.9	24
293	Computer-aided detection of clustered microcalcifications on digital mammograms. Medical and Biological Engineering and Computing, 1995, 33, 174-178.	2.8	92
294	Analysis of spiculation in the computerized classification of mammographic masses. Medical Physics, 1995, 22, 1569-1579.	3.0	155
295	Automated segmentation of digitized mammograms. Academic Radiology, 1995, 2, 1-9.	2.5	120
296	Effect of case selection on the performance of computer-aided detection schemes. Medical Physics, 1994, 21, 265-269.	3.0	129
297	Computerized detection of clustered microcalcifications in digital mammograms using a shift-invariant artificial neural network. Medical Physics, 1994, 21, 517-524.	3.0	145
298	Computerized detection of abnormal asymmetry in digital chest radiographs. Medical Physics, 1994, 21, 1761-1768.	3.0	19
299	Digital image subtraction of temporally sequential chest images for detection of interval change. Medical Physics, 1994, 21, 453-461.	3.0	190
300	Multifractal radiographic analysis of osteoporosis. Medical Physics, 1994, 21, 503-508.	3.0	158
301	Computerized detection of masses in digital mammograms: Investigation of feature-analysis techniques. Journal of Digital Imaging, 1994, 7, 18-26.	2.9	22
302	Development of a digital duplication system for portable chest radiographs. Journal of Digital Imaging, 1994, 7, 146-153.	2.9	6
303	Reduction of false positives in computerized detection of lung nodules in chest radiographs using artificial neural networks, discriminant analysis, and a rule-based scheme. Journal of Digital Imaging, 1994, 7, 196-207.	2.9	49
304	Computerized detection of masses in digital mammograms: Automated alignment of breast images and its effect on bilateral-subtraction technique. Medical Physics, 1994, 21, 445-452.	3.0	125
305	Computerized characterization of mammographic masses: analysis of spiculation. Cancer Letters, 1994, 77, 201-211.	7.2	52
306	Computerized Detection of Pulmonary Nodules in Computed Tomography Images. Investigative Radiology, 1994, 29, 459-465.	6.2	180

#	Article	IF	CITATIONS
307	Simulation studies of data classification by artificial neural networks: Potential applications in medical imaging and decision making. Journal of Digital Imaging, 1993, 6, 117-125.	2.9	20
308	Automatic segmentation of liver structure in CT images. Medical Physics, 1993, 20, 71-78.	3.0	125
309	Development of a high quality film duplication system using a laser digitizer: Comparison with computed radiography. Medical Physics, 1993, 20, 51-58.	3.0	17
310	Computer-aided detection of clustered microcalcifications: An improved method for grouping detected signals. Medical Physics, 1993, 20, 1661-1666.	3.0	53
311	<title>Computer-aided detection and diagnosis of masses and clustered microcalcifications from digital mammograms</title> . , 1993, , .		25
312	Comparison of Bilateral-Subtraction and Single-Image Processing Techniques in the Computerized Detection of Mammographic Masses. Investigative Radiology, 1993, 28, 473-481.	6.2	86
313	Computer-Aided Diagnosis in Chest Radiography Preliminary Experience. Investigative Radiology, 1993, 28, 987-993.	6.2	28
314	High-Quality Portable Chest Images Using Enhanced Film-Digitization and Computed Radiography. , 1993, , 447-449.		0
315	<title>Application of artificial neural networks in mammography for the diagnosis of breast cancer</title> . , 1992, 1778, 19.		4
316	Computerized detection of clustered microcalcifications in digital mammograms: Applications of artificial neural networks. Medical Physics, 1992, 19, 555-560.	3.0	132
317	Application of the EM algorithm to radiographic images. Medical Physics, 1992, 19, 1175-1182.	3.0	15
318	<title>Method of extracting signal area and signal thickness of microcalcifications from digital mammograms</title> ., 1992, , .		14
319	<title>User interface optimization in a radiography display console</title> . , 1992, 1654, 432.		3
320	Potential Usefulness of Computerized Nodule Detection in Screening Programs for Lung Cancer. Investigative Radiology, 1992, 27, 471-475.	6.2	39
321	Image Feature Analysis of False-Positive Diagnoses Produced by Automated Detection of Lung Nodules. Investigative Radiology, 1992, 27, 587-597.	6.2	75
322	Computerized Scheme for the Detection of Pulmonary Nodules. Investigative Radiology, 1992, 27, 124-129.	6.2	42
323	<title>Development of a smart workstation for use in mammography</title> . , 1991, 1445, 101.		11
324	Comparison of imaging properties of a computed radiography system and screen-film systems. Medical Physics, 1991, 18, 414-420.	3.0	30

19

#	Article	IF	CITATIONS
325	Computerized detection of masses in digital mammograms: Analysis of bilateral subtraction images. Medical Physics, 1991, 18, 955-963.	3.0	181
326	6. COMPARISON OF IMAGING PROPERTIES OF A COMPUTED RADIOGRAPHY SYSTEM AND SCREEN-FILM SYSTEMS EVALUATED IN THE UNIVERSITY OF CHICAGO. Japanese Journal of Radiological Technology, 1991, 47, 870-874.	0.1	0
327	<title>Investigation of methods for the computerized detection and analysis of mammographic
masses</title> . Proceedings of SPIE, 1990, , .	0.8	44
328	Computer-aided diagnosis in chest radiology. Journal of Thoracic Imaging, 1990, 5, 67-76.	1.5	56
329	<title>Neural network approach for differential diagnosis of interstitial lung
diseases</title> . Proceedings of SPIE, 1990, 1233, 45.	0.8	8
330	Measurement of the presampling modulation transfer function of film digitizers using a curve fitting technique. Medical Physics, 1990, 17, 962-966.	3.0	61
331	Computerized detection of pulmonary nodules in digital chest images: Use of morphological filters in reducing false-positive detections. Medical Physics, 1990, 17, 861-865.	3.0	84
332	Investigation of basic imaging properties in digital radiography. 13. Effect of simple structured noise on the detectability of simulated stenotic lesions. Medical Physics, 1989, 16, 14-21.	3.0	32
333	Digitized Film Radiography. Investigative Radiology, 1989, 24, 910-916.	6.2	12
334	Image feature analysis and computer-aided diagnosis in digital radiography. 3. Automated detection of nodules in peripheral lung fields. Medical Physics, 1988, 15, 158-166.	3.0	218
335	Investigation of basic imaging properties in digital radiography. 12. Effect of matrix configuration on spatial resolution. Medical Physics, 1988, 15, 384-390.	3.0	6
336	<title>Computerized Detection Of Lung Nodules In Digital Chest Radiographs</title> . Proceedings of SPIE, 1987, , .	0.8	17
337	Basic Imaging Properties of a Large Image Intensifier-TV Digital Chest Radiographic System. Investigative Radiology, 1987, 22, 328-335.	6.2	31
338	Effect of pixel size on detectability of low-contrast signals in digital radiography. Journal of the Optical Society of America A: Optics and Image Science, and Vision, 1987, 4, 966.	1.5	18
339	Investigation of basic imaging properties in digital radiography. 7. Noise Wiener spectra of II-TV digital imaging systems. Medical Physics, 1986, 13, 131-138.	3.0	56
340	Investigation of basic imaging properties in digital radiography. 8. Detection of simulated low-contrast objects in digital subtraction angiographic images. Medical Physics, 1986, 13, 304-311.	3.0	22
341	Investigation of basic imaging properties in digital radiography. 9. Effect of displayed grey levels on signal detection. Medical Physics, 1986, 13, 312-318.	3.0	9
342	Investigation of basic imaging properties in digital radiography. 10. Structure mottle of II-TV digital imaging systems. Medical Physics, 1986, 13, 843-849.	3.0	19

#	Article	IF	CITATIONS
343	Investigation of basic imaging properties in digital radiography. 5. Characteristic curves of II-TV digital systems. Medical Physics, 1986, 13, 13-18.	3.0	28
344	Investigation of basic imaging properties in digital radiography. 6. MTFs of II-TV digital imaging systems. Medical Physics, 1985, 12, 713-720.	3.0	94
345	Investigation of basic imaging properties in digital radiography. 3. Effect of pixel size on SNR and threshold contrast. Medical Physics, 1985, 12, 201-208.	3.0	44
346	Investigation of basic imaging properties in digital radiography. I. Modulation transfer function. Medical Physics, 1984, 11, 287-295.	3.0	142
347	Investigation of basic imaging properties in digital radiography. 2. Noise Wiener spectrum. Medical Physics, 1984, 11, 797-805.	3.0	134
348	Quantitative breast image analysis for personalized medicine. SPIE Newsroom, 0, , .	0.1	0
349	Computer-Aided Diagnosis in Mammography. , 0, , 915-1004.		55
350	Comment on "Machine Learning for Early Detection of Hypoxic-Ischemic Brain Injury After Cardiac Arrest―Submitted by Noah Salomon Molinski et al Neurocritical Care, 0, , .	2.4	0